UNIVERSITYOF BIRMINGHAM

University of Birmingham
Research at Birmingham

VEGF induces signalling and angiogenesis by directing VEGFR2 internalisation via macropinocytosis

Basagiannis, Dimitris; Murphy, Carol; Mercer, Jason

Document Version
Peer reviewed version

[Link to publication on Research at Birmingham portal](#)

VEGF induces signalling and angiogenesis by directing VEGFR2 internalisation via macropinocytosis.

Running title: Endocytic routes of VEGFR2

Dimitris Basagiannis[1,2], Sofia Zografou[1], Carol Murphy[1,3], Theodore Fotsis[1,2], Lucia Morbidelli[4], Marina Ziche[4], Christopher Bleck[5], Jason Mercer[5,6], and Savvas Christoforidis[1,2,*]

[1]Institute of Molecular Biology and Biotechnology-Biomedical Research, Foundation for Research and Technology, 45110 Ioannina, Greece
[2]Laboratory of Biological Chemistry, Department of Medicine, School of Health Sciences, University of Ioannina, 45110 Ioannina, Greece
[3]School of Biosciences, College of Life and Environmental Sciences, University of Birmingham, Edgbaston, Birmingham, B15 2TT, UK
[4]Department of Life Sciences, University of Siena, Via Aldo Moro 2, 53100, Siena, Italy
[5]Institute of Biochemistry, ETH Zurich, Switzerland.
[6]MRC-Laboratory for Molecular Cell Biology, University College London, Gower Street, London WC1E 6BT, UK

*Correspondence should be addressed to S.C. (e-mail: savvas_christoforidis@imbb.forth.gr, schristo@uoi.gr)

keywords: endocytosis, macropinocytosis, membrane trafficking, signalling, VEGF, VEGFR2

1

SUMMARY STATEMENT

VEGFR2 internalises constitutively via clathrin-mediated endocytosis, while VEGF introduces a new internalisation itinerary for VEGFR2, the pathway of macropinocytosis, which is essential for VEGF signalling and angiogenesis.

ABSTRACT

Endocytosis plays critical role in receptor signalling. VEGFR2 and its ligand VEGFA are fundamental in neovascularization. Yet, our understanding of the role of endocytosis in VEGFR2 signalling remains limited. Despite the existence of diverse internalisation routes, the only known endocytic pathway of VEGFR2 is the clathrin-mediated. Here, we show that this pathway is the predominant internalisation route of VEGFR2 only in the absence of ligand. Intriguingly, VEGF introduces a novel internalisation itinerary for VEGFR2, the pathway of macropinocytosis, which becomes the prevalent endocytic route of the receptor in the presence of ligand, while the route of clathrin becomes minor. Macropinocytic internalisation of VEGFR2, which mechanistically is mediated via the small GTPase CDC42, takes place via macropinosomes generated at ruffling areas of the membrane. Interestingly, macropinocytosis plays critical role in VEGF-induced signalling, endothelial cell functions in vitro and angiogenesis *in vivo*, while clathrin-mediated endocytosis is not essential for VEGF signalling. These findings expand our knowledge on the endocytic pathways of VEGFR2 and suggest that VEGF-driven internalisation of VEGFR2 via macropinocytosis is essential for endothelial cell signalling and angiogenesis.

INTRODUCTION

It has been originally thought that the plasma membrane is the exclusive place from where the ligand/receptor complexes activate downstream signalling cascades. In this view, endocytosis was considered to cause termination of signalling via directing the receptors to lysosomes for degradation. However, it is now evident that a number of receptors explore the endocytic routes in order to tune the duration, amplitude and specificity of the signalling process (McMahon and Boucrot, 2011; Miaczynska et al., 2004; Sorkin and von Zastrow, 2009).

VEGFR2 is a major angiogenic receptor that plays crucial role in blood vessel homeostasis and vascular diseases (Herbert and Stainier, 2011; Olsson et al., 2006). Additionally, VEGFR2-triggered angiogenesis is a hallmark of cancer progression and metastasis (Herbert and Stainier, 2011; Olsson et al., 2006). Numerous previous studies

have contributed to a remarkable knowledge regarding the signalling cascades that are activated by VEGF and their importance in VEGF-mediated functions. Yet, our understanding on the different routes that are responsible for VEGFR2 internalisation remains limited. Thus, until now, the only known endocytic route for VEGFR2 is the canonical clathrin-mediated pathway (Bhattacharya et al., 2005; Bruns et al., 2010; Bruns et al., 2012; Ewan et al., 2006; Gourlaouen et al., 2013; Lampugnani et al., 2006; Lee et al., 2014; Nakayama et al., 2013; Pasula et al., 2012; Sawamiphak et al., 2010; Tessneer et al., 2014), while its importance in VEGF signalling is debated (Bruns et al., 2010; Gourlaouen et al., 2013; Lampugnani et al., 2006; Lee et al., 2014; Pasula et al., 2012; Tessneer et al., 2014). Intriguingly, VEGF-induced degradation of VEGFR2 persisted despite inhibition of clathrin mediated endocytosis (Bhattacharya et al., 2005; Fearnley et al., 2016; Gourlaouen et al., 2013; Pasula et al., 2012; Tessneer et al., 2014), thereby suggesting that the receptor may also internalise via clathrin-independent endocytic routes, a possibility that remains unexplored.

To unambiguously address the role of endocytosis in VEGFR2 function, here we identified the different endocytic itineraries of VEGFR2 and tested their functional significance in signalling. Our findings suggest that clathrin-mediated endocytosis is the main endocytic route of VEGFR2 only in the absence of ligand, while addition of VEGF introduces a novel internalisation itinerary for VEGFR2, the route of macropinocytosis, which is essential for VEGF signalling, endothelial cell functions and angiogenesis.

RESULTS
Although constitutive internalisation of VEGFR2 is clathrin-mediated, VEGF introduces a novel, clathrin-independent internalisation route for the receptor.
To systematically analyse the internalisation routes of VEGFR2, we studied the pathways of endocytosis both in the absence of ligand (constitutive, steady state internalisation) and in the presence of VEGFA, in primary endothelial cells (HUVECs). The isoform of VEGF used throughout the present study is VEGF165a, the most well studied ligand of VEGFR2 (Olsson et al., 2006), thereafter called simply VEGF. To track the internalization itineraries of VEGFR2, at first we employed a microscopy-based anti-VEGFR2 antibody uptake assay in live cells (Gourlaouen et al., 2013; Lampugnani et al., 2006; Sawamiphak et al., 2010), followed by an acid-wash step to strip the antibody that remains associated to the plasma membrane (this method does not interfere with VEGF signalling and VEGFR2 phosphorylation, data not shown). Given that, apart from plasma membrane localization, a significant amount of VEGFR2 is localized at the Golgi and endosomal compartments (Gampel et al., 2006; Manickam et al., 2011), this assay allows detection of the molecules of the newly internalised receptor, excluding the interference form the intracellular or non-

internalised pools of VEGFR2. Using this experimental approach, we confirmed that VEGFR2 internalises even in the absence of VEGF, in a clathrin-dependent manner (Fig. 1A) (Basagiannis and Christoforidis, 2016; Ewan et al., 2006). However, unlike constitutive endocytosis, VEGF-stimulated internalisation of VEGFR2 was, unexpectedly, only partially inhibited by the knockdown of CHC (Fig. 1B) (similar data were obtained by a second siRNA against CHC, Fig. S1A). These data were confirmed by an independent methodological approach, which is based on a biotin-pull down assay that detects the remaining VEGFR2 at the cell surface, post-VEGF activation. By employing this technique, we found that VEGF causes an increase of the amount of internalised VEGFR2, while CHC knockdown was unable to substantially interfere with the uptake of the receptor (Fig. 1C). To further evaluate the contribution of CME in VEGF-induced internalisation, we developed, based on previous reports (Bator and Reading, 1989; Smith et al., 1997), an "ELISA-like" assay that assesses quantitatively the levels of VEGFR2 at the cell surface. In line with the above data, knockdown of CHC reduced only partially the uptake of the receptor (Fig. 1D), which suggests that VEGF induces a clathrin-independent route of internalisation for VEGFR2. Endocytosis via caveolae (plasma membrane invaginations, where VEGFR2 had been found to be localized (Lajoie and Nabi, 2010; Mayor and Pagano, 2007; Parton and del Pozo, 2013; Pelkmans et al., 2004; Shvets et al., 2014)) is not responsible for this new route of internalisation, since, knock down of caveolin-1 had no effect on VEGF-induced endocytosis of VEGFR2 (Fig. 1C, D).

To further test the contribution of CME in VEGF-induced endocytosis of VEGFR2, we investigated the involvement of dynamin 2, a well-established mediator of this pathway (Sever et al., 2000). Knockdown of dynamin 2 had no effect on the internalization of VEGFR2, as revealed by the microscopy- or the biotinylation- based approach (Fig. S1B and S1C, respectively). Furthermore, knockdown of either dynamin 2 or CHC had no substantial effect on VEGF-induced degradation of VEGFR2 (Fig. S1D), which is in line with the conclusion that internalization (and further degradation) of VEGFR2 takes place in a dynamin- and clathrin-independent manner.

The above data, which suggested that constitutive internalization of VEGFR2 is mediated via clathrin while VEGF induces a clathrin-independent route of internalisation, were further supported using TIRF-M in live cells expressing VEGFR2-mCherry. In the absence of VEGF, addition of dynasore, a rapidly acting inhibitor of dynamin (Macia et al., 2006), that blocks both clathrin and caveolae-mediated internalisation, led to an increase of VEGFR2 levels at the cell surface (compare left and middle images of Fig. S1E, see also Movie S1). Addition of VEGF caused a loss of the cell surface signal, suggesting that VEGF introduces a dynamin-independent route of entry (compare right and middle images of Fig. S1E, see also Movie S1). Combined, the above data suggest that, although in the absence

of ligand the receptor internalises mainly clathrin-dependently, VEGF introduces a novel, clathrin-independent route of internalisation for VEGFR2.

VEGF induces membrane ruffling and internalisation of VEGFR2 via macropinocytosis.

A hint about the identity of the new clathrin-independent route of VEGFR2 came from the observation that, following activation by VEGF, the size of a significant number of VEGFR2-positive endosomes was considerably larger than the size of endosomes carrying constitutively internalised VEGFR2 (presented in detail in the subsequent figures). A route that is well-known for generating large endocytic vesicles is macropinocytosis (Kerr and Teasdale, 2009; Mayor and Pagano, 2007; Mercer and Helenius, 2009). To test whether VEGF induces macropinocytic internalisation of VEGFR2, as well as to exclude the possibility that the clathrin-independent internalisation of the receptor is due to the induction of compensatory endocytic pathways (Damke et al., 1995) (as a consequence of the long-term inhibition of CME), we employed a number of experiments, in the absence of any perturbation of endocytic routes. First, given that macropinocytosis initiates at sites where membrane ruffling and actin reorganization takes place (Kerr and Teasdale, 2009), we employed dual color video microscopy to analyse the spatio-temporal coordination of the cell membrane dynamics (followed by GFP-actin) with receptor endocytosis (monitored by VEGFR2-mCherry). Interestingly, upon activation with VEGF, we observed sites of the membrane undergoing intense membrane ruffling (seen by the dynamics of GFP-actin), followed by the formation of large vesicles that were positive for both actin and VEGFR2 (see Movie S2 and Fig. 2A). Actin was only transiently present at these vesicles, that is, from the beginning of their generation until they were fully formed. Second, we quantified the size, the number and the fluorescence intensity of the vesicles containing VEGFR2, in quiescent and VEGF-stimulated cells. Interestingly, VEGF caused a striking increase of the content of VEGFR2 (relative fluorescence of VEGFR2) in large sized vesicles along with an increase of the number of these vesicles (Fig. 2B). Third, as a complementary approach, we analysed by electron microscopy the morphology and the size of vesicles containing VEGFR2. In VEGF-activated cells, there was a significant increase over time of the signal of VEGFR2 (number of gold particles) in vesicles whose size was over 0.2 μm (Fig. 2C).

Subsequently, fourth, we tested the colocalization of internalised VEGFR2 with known markers of macropinosomes. Induction by VEGF led to internalisation of VEGFR2 in endosomes that were positive for high-molecular mass dextran (Fig. 3A), an established cargo/marker of macropinosomes (Mercer and Helenius, 2009; Schnatwinkel et al., 2004). Additionally, VEGFR2 colocalized with Rabankyrin-5 (Fig. 3A), an endosomal protein that, besides being localized to diverse endocytic vesicles (Fabrowski et al., 2013; Ishii et al.,

2003; Schnatwinkel et al., 2004; Zhang et al., 2012), also localizes to macropinosomes (Schnatwinkel et al., 2004). We also tested the colocalization of internalized VEGFR2 with EEA1, a marker of the early endosomes (Mu et al., 1995). Triple labeling analysis revealed that a number of vesicles double-positive for VEGFR2 and Rabankyrin-5 were either negative or only poorly stained for EEA1 (Fig. S2), which is consistent with previous findings showing that macropinosomes are only weakly or not at all EEA1-positive (Schnatwinkel et al., 2004). Notably, given that the above four independent experimental approaches (Figs 2A, B, C, 3A, and movie S1) are employed in the absence of any perturbation of endocytosis, it is concluded that macropinocytosis of VEGFR2 is not a compensatory endocytic pathway that takes place as a consequence of the long-term inhibition of CME (Damke et al., 1995), but rather due to the ability of VEGF to induce macropinocytic internalisation of its receptor. Finally, fifth, we tested the effect of EIPA, a commonly used inhibitor of macropinocytosis (Commisso et al., 2014; Kerr and Teasdale, 2009; Koivusalo et al., 2010; Kuhling and Schelhaas, 2014), on VEGF-induced internalisation of VEGFR2. Treatment with EIPA caused a substantial decrease of endocytosis of both VEGFR2 and dextran, as well as a reduction of the number of the large VEGFR2-positive vesicles (Fig. 3B), while internalization in small vesicles was not substantially affected (Fig. 3B). Concomitant treatment with EIPA and dynasore resulted in an almost complete inhibition of the internalization of VEGFR2 in large as well as in small vesicles (Fig. 3B), suggesting that, while macropinocytosis is the main internalization route of VEGFR2, a fraction of the receptor is internalized via CME. To quantify the relative contribution of macropinocytosis and CME in VEGFR2 internalisation, we employed the "ELISA-like" assay described above, which determines the surface levels of VEGFR2 in intact cells. We found that the inhibitory effect of EIPA was approximately 2-fold higher than that of dynasore (EIPA and dynasore inhibited internalisation by 70% and 30%, respectively), and that the two inhibitors together blocked completely the uptake of the receptor, suggesting that CME and macropinocytosis are the sole routes of VEGFR2 internalisation (Fig. 3C). Thus, several lines of evidence suggest that, upon induction with VEGF, macropinocytosis accounts for approximately 70% of VEGFR2 internalisation while only 30% of the receptor is internalised via CME (Figs 1B-D, 3C). Based on all the above, macropinocytosis emerges here as a novel route of VEGF-induced entry of VEGFR2, which, although operates in parallel to CME, is the prefered endocytic route of this receptor.

Macropinocytosis of VEGFR2 is mediated by the small GTPase CDC42.
To get insights into the mechanism of macropinocytosis of VEGFR2, as well as to further validate the macropinocytic internalization of this receptor, we tested the involvement of the small GTPase CDC42, a known regulator of macropinocytosis (Chen et al., 1996; Fiorentini

et al., 2001; Garrett et al., 2000; Koivusalo et al., 2010). Indeed, treatment of HUVECs with siRNAs against CDC42 inhibited internalization of both high MW dextran (known cargo of macropinocytosis) and VEGFR2 (Fig. 4A). Additionally, using the biochemical biotinylation assay, we found that knockdown of CDC42 attenuated the uptake of the receptor (Fig. 4B). Finally, interference with CDC42 delayed significantly VEGF-induced degradation of VEGFR2 (Fig. 4C). These data not only suggest that the mechanism of macropinocytosis of VEGFR2 involves the function of the GTPase CDC42, but also further substantiate that this receptor is endocytosed via macropinocytosis.

Macropinocytosis is critical for VEGF signalling, endothelial cell functions and angiogenesis.

We then proceeded to address the significance of both CME and macropinocytosis, in VEGF-induced signalling and endothelial cell functions. Consistently with the minor contribution of CME (up to 30%) in VEGF-induced endocytosis of VEGFR2 (Figs 1B-D, 3C, S1A-C), inhibition of this route by knockdown of CHC had no effect on ERK1/2 or Akt phosphorylation (Fig. 5A) (similar data were obtained by a second siRNA against CHC, Fig. S3A). Likewise, interference with the function of dynamin, either by knockdown of dynamin 2 (Fig. 5B) or by overexpression of dynamin-K44A (Fig. S3B), had no substantial effect on ERK1/2 or Akt phosphorylation. A minor inhibition of Akt phosphorylation by overexpression of dynamin K44A (Fig. S3B) could be explained by the additional role of dynamin in signalling, independently from its well established function in vesicle budding (Fish et al., 2000)). Collectively, these data suggest that CME of VEGFR2 is not essential for VEGF-induced signalling.

Interestingly, in keeping with the predominant contribution of macropinocytosis in VEGFR2 internalisation (~70%, Fig. 3C), treatment with EIPA resulted in a robust inhibition of ERK1/2 and Akt phosphorylation (Fig. 6A, top panels). Furthermore, consistently with the involvement of CDC42 in VEGFR2 macropinocytosis (Fig. 4A-C), knockdown of this GTPase led to a substantial inhibition of VEGF-induced signalling (Fig. 6A, bottom panels). To further evaluate the importance of macropinocytosis in VEGF-mediated functions, we tested whether inhibition of macropinocytosis influences VEGF-induced endothelial cell properties. Indeed, inhibition of macropinocytosis by either EIPA or knockdown of CDC42 blocked VEGF-induced endothelial cell sprouting (Fig. 6B), migration (Fig. 6C and S4A) and survival (Fig. 6D), while knockdown of CHC or dynamin 2 had no substantial effect (Fig. 6B-D, S4A). Minor effects of the knockdown of dynamin (but not of CHC) in endothelial cell sprouting (Fig. 6B), or of the knockdown of CHC (but not of dynamin) in endothelial cell survival (Fig. 6D), could be due to an independent role of these trafficking regulators on the transport of critical molecules (other than VEGFR2), as proposed recently (Lee et al., 2014). Consistently with

this view, the knockdown of dynamin interfered with basal endothelial cell migration, without affecting the dependence on VEGF (Fig. 6C). Besides, the minor effect of CHC knockdown in cell survival (Fig. 6D) might be due to the fact that inhibition of CME causes a reduction of the levels of VEGFR2 (Fig. 1C, (Basagiannis and Christoforidis, 2016; Fearnley et al., 2016)).

Finally, in line with the above *in vitro* data, EIPA blocked VEGF-induced formation of new blood vessels in matrigel angiogenesis assays in mice (Fig. S4B), as well as in corneal neovascularisation assays in rabbits (Fig. S4C). Overall, these data suggest that macropinocytosis is critical for VEGF-induced signalling, endothelial cell functions and angiogenesis.

DISCUSSION

Here we found that the prefered internalisation itinerary of VEGFR2 upon induction with VEGF is distinct from the internalisation route that the receptor follows constitutively (see model in Fig. 7). Without ligand, VEGFR2 is mainly endocytosed in a clathrin-dependent manner, while, unexpectedly, VEGF switches the preference of the internalisation of VEGFR2 towards macropinocytosis, an endocytic route that is critical for downstream signalling to ERK1/2 and Akt, for endothelial cell functions and for angiogenesis *in vivo*.

To date, the sole known route of internalisation of VEGFR2 is the clathrin- and dynamin-mediated endocytosis (Bhattacharya et al., 2005; Bruns et al., 2010; Ewan et al., 2006; Gourlaouen et al., 2013; Lampugnani et al., 2006; Lee et al., 2014; Nakayama et al., 2013; Pasula et al., 2012; Sawamiphak et al., 2010; Tessneer et al., 2014). Yet, intriguingly, several studies reported that VEGFR2 degradation persists even when the pathway of clathrin is blocked (Bhattacharya et al., 2005; Fearnley et al., 2016; Gourlaouen et al., 2013; Pasula et al., 2012; Tessneer et al., 2014), which suggests that VEGFR2 is also internalised via a route that is independent from clathrin. Indeed, the data presented here suggest that, following activation with VEGF, the preferred route of endocytosis of VEGFR2 is macropinocytosis, while, unexpectedly, only a minor fraction of VEGFR2 internalises via CME. Several lines of evidence support the macropinocytic internalisation of VEGFR2. First, VEGF induces the formation of large VEGFR2 positive vesicles at areas undergoing pronounced membrane ruffling (observed by live-cell microscopy). Second, the size of these vesicles is compatible with the known large size of macropinosomes (estimated by either confocal or electron microscopy). Third, following activation with VEGF, internalised VEGFR2 colocalized with dextran and Rabankyrin-5. Finally, fourth, VEGFR2 internalisation was largely inhibited by EIPA, commonly used inhibitor of macropinocytosis (Commisso et al., 2014; Kerr and Teasdale, 2009; Koivusalo et al., 2010; Kuhling and Schelhaas, 2014), or by

knocking down the small GTPase CDC42, a well-characterized mediator of macropinocytosis (Chen et al., 1996; Fiorentini et al., 2001; Garrett et al., 2000; Koivusalo et al., 2010).

Our data suggest that CME is not required for VEGF signaling to ERK1/2 or to Akt, while macropinocytosis is critical. This finding is consistent with previous studies showing that CME is not essential for VEGF-mediated activation of the downstream signaling cascades (Bruns et al., 2010; Lampugnani et al., 2006; Lee et al., 2014; Pasula et al., 2012; Tessneer et al., 2014). Yet, in contrast to these data, other studies have reported that CME is required for VEGF-mediated downstream signaling (Gourlaouen et al., 2013; Nakayama et al., 2013). It is possible that these differences are due to the different employed techniques, tools or cell lines. In fact, differences in the importance of endocytosis between primary endothelial cells and transformed cell lines has been reported before (Gourlaouen et al., 2013). Additionally, a recent study proposed that reduced VEGF signaling upon depletion of CHC may be simply due to the enhanced degradation of VEGFR2, rather than due to a direct effect of this trafficking route in signaling (Fearnley et al., 2016). In any case, our findings are in line with the predominant and most recent view that CME is not required for VEGF signalling (Bruns et al., 2010; Lampugnani et al., 2006; Lee et al., 2014; Pasula et al., 2012; Tessneer et al., 2014). Thus, all in all, it appears that CME of VEGFR2 is not necessary for signalling to ERK1/2 ((Bruns et al., 2010; Lampugnani et al., 2006; Lee et al., 2014; Pasula et al., 2012; Tessneer et al., 2014) and present study) while macropinocytosis is absolutely essential (present study).

Since CME is the major route of constitutive endocytosis of VEGFR2 (in the absence of ligand), an appealing question raised from our findings is why does VEGF need to introduce a new route of internalisation for VEGFR2 (macropinocytosis). In other words, how could one explain that CME of VEGFR2, unlike macropinocytosis, is not able to support signalling? The inability of CME to support signalling could be either due to the lower efficiency of CME to internalise VEGFR2, or to its failure to co-internalise VEGFR2 with the necessary downstream molecules, or, finally, to the delivery of VEGFR2 to endosomal compartments that lack the appropriate downstream molecules. On the other hand, macropinocytosis may warrant VEGFR2 signalling by fulfilling one or more of the above functions. It is tempting to speculate that macropinocytosis might be responsible for delivering signalling complexes of the receptor to downstream targets, such as ERK1/2 and Akt, that may reside at specific endosomal compartments (Dobrowolski and De Robertis, 2012; McKay and Morrison, 2007; Miaczynska et al., 2004; Platta and Stenmark, 2011; Schenck et al., 2008; Sorkin and von Zastrow, 2009; Teis et al., 2002; Zouggari et al., 2009). Consequently, macropinocytosis could link VEGFR2 to downstream cascades required to regulate complex angiogenic responses, such as survival (Karali et al., 2014), proliferation and migration of endothelial cells (Herbert and Stainier, 2011).

A question that emerges from the present study is whether there are cellular conditions that affect macropinocytosis of VEGFR2, thereby influencing signaling, as well as whether macropinocytosis is the only route regulating the output of VEGFR2? Several observations provide the means to approach this issue. Different isoforms of VEGFA ligands (VEGF165, VEGF145, and VEGF121) have been found to exert differential effects on VEGFR2 signal transduction, trafficking and proteolysis (Ballmer-Hofer et al., 2011; Fearnley et al., 2016). Furthermore, VEGFR2 co-receptors, or other VEGFR2 interacting proteins, co-internalize with - and/or regulate the trafficking properties of - VEGFR2 (Ballmer-Hofer et al., 2011; Chen et al., 2010; Holmes and Zachary, 2008; Koch et al., 2014; Lampugnani et al., 2006; Lanahan et al., 2013; Lanahan et al., 2010; Nakayama et al., 2013; Salikhova et al., 2008; Sawamiphak et al., 2010). Thus, it is possible that different VEGF ligands may promote a differential association between VEGFR2 and its co-receptors/interacting partners, which may alter the balance between CME and macropinocytosis of VEGFR2, or may even introduce additional internalization routes for the receptor. These processes could control the diverse functions of the different types of endothelial cells, in different tissues, throughout the different stages of development, a hypothesis that warrants future investigations.

In the last years, macropinocytosis emerges as a critical endocytic route for the function of growth factors that play essential role in the vascular tissue, i.e. FGF2 (Elfenbein et al., 2012), PDGF (Schmees et al., 2012) and VEGF (present study). Thus, given that inhibition of macropinocytosis resulted in a robust inhibition of VEGF-induced angiogenesis in mice (present study), interference with macropinocytosis opens new perspectives in anti-angiogenic cancer therapy or other angiogenesis-related diseases.

MATERIALS AND METHODS

Reagents and antibodies. The concentration of the reagents used in this study, unless stated otherwise, is shown below in parentheses. Recombinant human VEGFA$_{165}$ (50 ng/ml) was obtained from Immunotools whereas dynasore (100 µmol/L) and 5-N-Ethyl-N-isopropyl amiloride (EIPA) (50 µmol/L) were from Sigma-Aldrich. Mouse and rabbit anti-VEGFR2 monoclonal antibodies were from Abcam (ab9530, 1:100) and Cell Signaling (#2479, 1:2000), respectively. The anti-actin antibody was from Millipore (MAB1501, 1:2000). Rabbit polyclonal antibodies against Early Endosome Antigen 1 (EEA1) and Rabankyrin-5 were kindly provided by Marino Zerial (MPI-CBG, Dresden, Germany). The anti-clathrin heavy chain antibody was from BD Biosciences (610499, 1:3000) whereas the anti-caveolin-1 (sc-894, 1:1000) and anti-CDC42 (sc-87, 1:200) antibodies were from Santa Cruz Biotechnology. The antibodies against p-VEGFR2 (Tyr1175) (#2478, 1:1000) ERK1/2 (#4695, 1:3000), p-ERK1/2 (#4370, 1:3000), Akt (#9272, 1:1000) and p-Akt (#4060, 1:1000), were from Cell

Signaling. Secondary antibodies coupled to Alexa fluorophores were from Invitrogen (1:400), while the HRP conjugated antibodies were from Jackson Immunoresearch (1:1000). All other reagents were obtained from Sigma-Aldrich, unless stated otherwise.

siRNAs, cDNAs and lentiviruses. The siRNAs for human clathrin heavy chain (5'GGGUGCCAGAUUAUCAAUUtt3' and 5'GGGAAGUUACAUAUUAUUGtt3') were from Ambion whereas the siRNAs for human CDC42 (5'GAUUACGACCGCUGAGUUA3') were from Dharmacon. The siRNAs for human dynamin-2 (5'CAUGCCGAGUUUUUGCACU553'), human caveolin-1 (5'AAGAGCUUCCUGAUUGAGAtt3') and control siRNAs (Random DS) were from Biospring. CDC42 and dynamin-2 knockdown experiments were carried out using 20 nmol/L of siRNAs. All other knockdown experiments were carried out using 50 nmol/L of siRNAs. Cells treated with siRNAs were assayed 60-72h post-transfection.

The cDNA of human VEGFR2 was kindly provided by Jacques Huot (Centre de Recherche du CHU de Québec, Canada). The VEGFR2-mCherry expression plasmid was generated by sub-cloning the cDNA of human VEGFR2 in pCMV-mCherry expression vector with standard cloning procedures.

Lentiviruses of dynamin wt (1 and 2) or dynamin K44A (1 and 2) were generated according to a previously reported protocol (Tiscornia et al., 2006). The cDNAs of dynamin 1 and 2 (both wt and K44A) were kindly provided by Sandra Schmid (UT Southwestern, Dallas, Texas). HUVECs were transduced at 50% confluence, in cell growth medium supplemented with 8 µg/ml polybrene. The next day, medium was changed and cells were assayed 24-36h post-transduction. Transduction efficiency was determined by the fluorescence of GFP, whose expression is controlled by the same promoter as dynamin.

Cell treatments. HUVECs were isolated, cultured and transfected as previously described (Zografou et al., 2012). Cells were routinely tested for contamination. VEGF-dependent and -independent experiments were carried out using 2h serum deprived cells. Drug treatments were carried out in serum-free M199 medium. Prior to VEGF stimulation, cells were treated with vehicle (DMSO) or inhibitors, for 30 min.

Indirect immunofluorescence microscopy. HUVECs were cultured in 35-mm diameter plastic dishes (appropriate for microscopy, by Ibidi), coated with collagen type I. Indirect immunofluorescence and analysis by confocal microscopy was employed as previously described (Papanikolaou et al., 2011). Images were captured using a Leica TCS SP5 II scanning confocal microscope and a Leica 63X HCX PL APO 1.4 NA objective. Data were subsequently processed in LAS AF according to the manufacturer guidelines.

Microscopy based internalisation assays. To monitor the internalisation fate of endogenous, cell surface pool of VEGFR2, HUVECs that were starved for 2h were transferred to 4^0C and the medium was replaced with ice cold blocking buffer (1% BSA in serum-free M199 medium buffered with 20 mmol/L HEPES). After a 30 min pre-cooling step, cells were treated for 1h with 10 µg/ml of mouse anti-VEGFR2 extracellular domain antibodies. Cells were washed 3x with blocking buffer and transferred to 37^0C in pre-warmed MI99 medium supplemented with 1.5 mg/ml 70kDa dextran Texas-Red or 50 µg/ml Fluorescein isothiocyanate-conjugated transferrin (Invitrogen), in the presence or absence of VEGF. Cells were acid-washed twice (ice cold M199 medium, pH 2.0), fixed and processed for immunofluorescence microscopy. The above protocol was also applied to siRNAs treated cells. When inhibitors were used, following antibodies incubation, cells were treated with vehicle or inhibitors for 30 min at 4^0C.

Biotinylation-based internalisation assays. To assess biochemically the amount of internalised VEGFR2, 2h serum starved siRNAs treated HUVECs were stimulated with VEGF for 15 min, transferred to 4^0C and labeled with 0.5 mg/ml EZ-Link Sulfo-NHS-S-S-Biotin (Thermo-Scientific) at 4^0C, for 20 min. Unbound biotin was quenched with 50 mM glycine in PBS, cells were lysed in lysis buffer (0.5% Triton X-100, 0.5% NP-40, 50 mM Tris pH 7.5, 100 mM NaCl, 5 mM EDTA and Roche protease inhibitors cocktail) and processed for pull-down using streptavidin beads.

Total Internal Reflection Fluorescence Microscopy. Live cell imaging of plasma membrane VEGFR2 was accomplished by Total Internal Reflection Fluorescence Microscopy (TIRF-M). Cells were analysed using a Leica AM TIRF MC set up on a Leica DMI6000 B microscope and a Leica 100X HCX PL APO 1.4 NA objective.
For live cell TIRF-M analysis, the medium of HUVECs transfected with a VEGFR2-mCherry expression plasmid was replaced with microscopy solution, cells were transferred to a 37^0C chamber and analysed by TIRF-M (48h post-transfection). During analysis, dynasore and VEGF were added sequentially at the indicated time points.

Electron microscopy. HUVECs were stimulated with VEGF for 10 or 20 min and fixed in 4% formaldehyde and 0.1% glutaraldehyde in 1x PHEM buffer for 60-90 min. Cryo-sectioning and immuno-labelling was performed as described elsewhere (Schmidt et al., 2011). In brief, ultrathin sections (50–70 nm) from gelatin-embedded and frozen cell pellets were obtained using an FC7/UC7-ultramicrotome (Leica, Vienna, Austria). Immunogold labeling was carried out in thawed sections using rabbit anti-VEGFR2 cytoplasmic domain antibodies (1:20) and 5 nm protein A-gold (UMC Utrecht University, Utrecht, The Netherlands) (1:50). A mixture

of uranyl acetate and methyl cellulose was used for embedding and negative staining. Sections were examined using a CM10 Philips transmission electron microscope with an Olympus 'Veleta' 2kx2k side-mounted TEM CCD camera. For the counting of gold particles, we used the stereology method, by systematic uniform random sampling, in 2D space.

Surface VEGFR2 ELISA. Previous studies had developed protocols for the measurement of surface antigens using the cell-surface ELISA technique (Bator and Reading, 1989; Smith et al., 1997). Here we have established the conditions for the measurement of VEGFR2 on the surface of HUVECs. In brief, HUVECs cultured in 96-well dishes were treated with inhibitors, stimulated with VEGF for 30 min, washed 3x with PBS and fixed with 3.7% PFA for 20 min. Non-specific sites were blocked with 1% BSA in PBS (blocking buffer) for 1h. Cells were incubated for 2h with goat anti-VEGFR2 extracellular domain antibodies (R&D Systems, AF357, 1.5 µg/ml in blocking buffer), washed 5X with blocking buffer and treated with anti-goat horseradish peroxidase-coupled secondary antibodies, for 1h. Subsequently, the cells were washed 5X and the reaction was initiated by the addition of 250 µl of substrate buffer (20 mg o-phenylenediamine in 50 ml phosphate-citrate buffer, pH 5.0, supplemented with 20 µl H_2O_2 30%). The reaction was terminated by the addition of 50 µl H_2SO_4 2 mol/L and the absorbance was measured at 492 nm. Measured values were normalized according to the total protein of samples that were treated in parallel and lysed before the fixation step of the assay. For siRNA experiments, cells were cultured and transfected in 24-well dishes. 48h post-transfection, cells were detached using trypsin, seeded confluent in 96-well plates and assayed after 24h. Non-stimulated cells were processed in parallel.

Spheroid sprouting, migration and MTT assays. The generation of HUVEC spheroids was performed according to a previously described protocol (Korff and Augustin, 1999). Briefly, siRNAs treated cells were trypsinized 24h post-transfection and HUVEC spheroids were generated using defined number of cells (600 cells), for 24h, in hanging drops cultures, in cell growth medium supplemented with 0.24% w/v carboxylmethylcellulose. Spheroids were harvested and embedded in 500 µl of rat type I collagen gels (supplemented with M199 medium, 10% FCS and 0.24% w/v carboxylmethylcellulose) and were stimulated with 50 ng/ml VEGF (in 100 µl of M199 medium, on top of the gels), for 16h. In the case of EIPA treatment, EIPA (50 µM) was added to the gels in combination with VEGF. Images of spheroids were captured via a Leica DMI6000 B microscope and spheroid sprouting was analyzed using ImageJ software.

Migration of endothelial cells was assessed via the wound healing assay. Confluent HUVEC monolayers grown in 24-well plates were serum-starved for 6h in M199 medium supplemented with 2% FCS and linear scratch injuries were applied with a 200 µl plastic

pipette tip. Cells were washed 3x with HBSS and treated with 50 ng/ml VEGF in serum starvation medium, for 14h. Non-stimulated cells were analysed in parallel. In the case of treatment with EIPA, cells were pre-incubated with 50 µM EIPA for 30 min, prior to the addition of VEGF. Images of random injury areas were acquired at 0 and 14h using a Leica DMI6000 B microscope. Migration of endothelial cells was analyzed using the ImageJ software.

Survival of endothelial cells was determined by the MTT assay. 24h post-transfection, siRNAs treated HUVECs were trypsinized and seeded in 96-well plates at a density of $6x10^3$ cells. Next day, cells were serum starved for 24h in M199 medium supplemented with 2% FCS. Then, the media were supplemented with 50 ng/ml VEGF (VEGF was replenished every 24h) and cells were incubated for 48h. At the end of the incubation, cells were treated with 0.5 mg/ml 3-(4, 5-dimethylthiazol-2-yl)-2, 5-diphenyltetrazolium bromide (MTT), for 4h, at 37°C. Then, the media were aspirated and formazan crystals were dissolved by the addition of 200 µl of DMSO. Subsequently, plates were agitated gently and the optical density was measured at 570nm. VEGF-untreated cells were analyzed in parallel.

***In vivo* Matrigel and rabbit cornea angiogenesis assay.** Animal experiments have been performed in accordance with the guidelines of the European Commission for animal care and welfare (Directive 2010/63/EU) and the local and national ethical committees.

The Matrigel plug assay was employed as described before (Finetti et al., 2008). VEGF, in the presence of EIPA, was diluted in Matrigel (Becton Dickinson, growth factors and phenol red-free) on ice. Final drug concentrations were 500 ng/plug VEGF and 50 µmol/L EIPA. C57/B6J mice (12 week old, 15 animals in total) were subcutaneously injected in the dorsal midline region with 0.4 mL of Matrigel alone or with Matrigel containing the stimuli. After 7 days, the mice were euthanized and implants were harvested. Plugs were re-suspended in 1 ml of Drabkin's reagent (Sigma), for 18h on ice, and haemoglobin concentration was determined by absorbance at 540 nm and compared with a standard curve (Sigma).

Angiogenesis was studied in the cornea of male New Zealand white rabbits (n=8, Charles River) as described (Monti et al., 2013). Animals were anesthetized by i.m. injection of xilazine 2% (0.5 ml/animal) andtiletamine/zolazepam (10 mg/kg). The depth of anesthesia was checked as reflex to pressure. Each eye was enucleated by the use of a dental dam, and a local anesthetic (i.e. 0.4% benoxinate) was instilled on the ocular surface just before surgery. The pellet implantation procedure started with a linear intrastromal incision using a surgical blade. The preparation of the corneal pocket for the pellet implant was made in the lower half of the cornea with a 1.5 mm pliable silver spatula with smooth edge blade. Pellets were implanted at 2 mm from the limbus to avoid false positives due to mechanical stress

and to favor gradient diffusion of test substances in the tissue toward the endothelial cells at the limbal plexus. To test the effect of EIPA (12,5 μg/pellet), a fully competent dose of VEGF (200 ng/pellet) was administered in the presence of the inhibitor, being the two substances released from separate and adjacent pellets. The corneas were observed, and digital images were taken by means of a slit-lamp stereomicroscope.

Quantifications. The quantification of immunoblots and immunofluorescence images was performed using the ImageJ software. For the analysis of the number and the size of VEGFR2-positive vesicles, vesicles were categorized in groups based on their size, where each group should contain at least 10 vesicles, in VEGF stimulated cells. For in vivo experiments, angiogenic score (number of progressing vessels/mm^2) was calculated during time in a blind manner by the use of ImageJ. In the case of EM experiments, for each time point (10 and 20 min, 3 times each, on 2 different sample grids), a total number of 250 gold particles were counted by meandering scanning. 5 cell components were assumed (plasma membrane, vesicles 0.2 μm<, vesicles >0.2 μm, nucleus, mitochondrion) for counting. In the ELISA-like assay of surface VEGFR2, an immobile fraction of VEGFR2 (40% of total), which does not internalise in the presence of VEGF, was excluded from all values.

Statistical analysis. Data plotting and statistical analysis was performed in GraphPad Prism. Statistical differences were evaluated using the student t-test, for two-group comparison, or analysis of variance (ANOVA) followed by Dunnett's post hoc analysis (one-way ANOVA) or Bonferroni post-tests analysis (two-way ANOVA), for comparisons of more than two groups. The values reported in the figures represent mean ± S.D. calculated from at least 3 replicates for each experimental setting.

Association for Cancer Research (AIRC grant n. IG10731 and IG15443) to MZ and Istituto
Toscano Tumori (ITT grant proposal 2010) to LM and MZ.

Competing interests

The authors state that they have no competing or financial interests.

AUTHOR CONTRIBUTIONS

D.B. and S.C. designed the study, and D.B. performed all the in vitro experiments. S.Z.
employed turnover and MTT assays and contributed in signalling assays and IF experiments.
L.M. and M.Z. carried out the *in vivo* experiments, analysed the data, prepared the
corresponding figures and wrote the relevant text. C.M. and T.F. provided transferrin and
anti-CDC42 antibodies and participated with ideas and critical discussions throughout this
work. C.B. and J.M. carried out and analysed the EM experiments, prepared the
corresponding figures and wrote the relevant text. D.B and S.C. wrote the paper. All authors
provided comments on the manuscript.

REFERENCES

Ballmer-Hofer, K., Andersson, A. E., Ratcliffe, L. E. and Berger, P. (2011). Neuropilin-1 promotes
   VEGFR-2 trafficking through Rab11 vesicles thereby specifying signal output. *Blood* **118**, 816-26.
Basagiannis, D. and Christoforidis, S. (2016). Constitutive Endocytosis of VEGFR2 Protects the
   Receptor Against Shedding. *J Biol Chem*.
Bator, J. M. and Reading, C. L. (1989). Measurement of antibody affinity for cell surface antigens
   using an enzyme-linked immunosorbent assay. *J Immunol Methods* **125**, 167-76.
**Bhattacharya, R., Kang-Decker, N., Hughes, D. A., Mukherjee, P., Shah, V., McNiven, M. A.
   and Mukhopadhyay, D.** (2005). Regulatory role of dynamin-2 in VEGFR-2/KDR-mediated
   endothelial signaling. *FASEB J* **19**, 1692-4.
**Bruns, A. F., Herbert, S. P., Odell, A. F., Jopling, H. M., Hooper, N. M., Zachary, I. C., Walker,
   J. H. and Ponnambalam, S.** (2010). Ligand-stimulated VEGFR2 signaling is regulated by co-
   ordinated trafficking and proteolysis. *Traffic* **11**, 161-74.
**Bruns, A. F., Yuldasheva, N., Latham, A. M., Bao, L., Pellet-Many, C., Frankel, P., Stephen, S.
   L., Howell, G. J., Wheatcroft, S. B., Kearney, M. T. et al.** (2012). A heat-shock protein axis
   regulates VEGFR2 proteolysis, blood vessel development and repair. *PLoS ONE* **7**, e48539.
Chen, L. M., Hobbie, S. and Galan, J. E. (1996). Requirement of CDC42 for Salmonella-induced
   cytoskeletal and nuclear responses. *Science* **274**, 2115-8.
Chen, T. T., Luque, A., Lee, S., Anderson, S. M., Segura, T. and Iruela-Arispe, M. L. (2010).
   Anchorage of VEGF to the extracellular matrix conveys differential signaling responses to
   endothelial cells. *J Cell Biol* **188**, 595-609.
Commisso, C., Flinn, R. J. and Bar-Sagi, D. (2014). Determining the macropinocytic index of cells
   through a quantitative image-based assay. *Nat Protoc* **9**, 182-92.
Damke, H., Baba, T., van der Bliek, A. M. and Schmid, S. L. (1995). Clathrin-independent
   pinocytosis is induced in cells overexpressing a temperature-sensitive mutant of dynamin. *J Cell
   Biol* **131**, 69-80.
Dobrowolski, R. and De Robertis, E. M. (2012). Endocytic control of growth factor signalling:
   multivesicular bodies as signalling organelles. *Nat Rev Mol Cell Biol* **13**, 53-60.

Elfenbein, A., Lanahan, A., Zhou, T. X., Yamasaki, A., Tkachenko, E., Matsuda, M. and Simons, M. (2012). Syndecan 4 regulates FGFR1 signaling in endothelial cells by directing macropinocytosis. *Sci Signal* **5**, ra36.

Ewan, L. C., Jopling, H. M., Jia, H., Mittar, S., Bagherzadeh, A., Howell, G. J., Walker, J. H., Zachary, I. C. and Ponnambalam, S. (2006). Intrinsic tyrosine kinase activity is required for vascular endothelial growth factor receptor 2 ubiquitination, sorting and degradation in endothelial cells. *Traffic* **7**, 1270-82.

Fabrowski, P., Necakov, A. S., Mumbauer, S., Loeser, E., Reversi, A., Streichan, S., Briggs, J. A. and De Renzis, S. (2013). Tubular endocytosis drives remodelling of the apical surface during epithelial morphogenesis in Drosophila. *Nat Commun* **4**, 2244.

Fearnley, G. W., Smith, G. A., Abdul-Zani, I., Yuldasheva, N., Mughal, N. A., Homer-Vanniasinkam, S., Kearney, M. T., Zachary, I. C., Tomlinson, D. C., Harrison, M. A. et al. (2016). VEGF-A isoforms program differential VEGFR2 signal transduction, trafficking and proteolysis. *Biol Open* **5**, 571-83.

Finetti, F., Solito, R., Morbidelli, L., Giachetti, A., Ziche, M. and Donnini, S. (2008). Prostaglandin E2 regulates angiogenesis via activation of fibroblast growth factor receptor-1. *J Biol Chem* **283**, 2139-46.

Fiorentini, C., Falzano, L., Fabbri, A., Stringaro, A., Logozzi, M., Travaglione, S., Contamin, S., Arancia, G., Malorni, W. and Fais, S. (2001). Activation of rho GTPases by cytotoxic necrotizing factor 1 induces macropinocytosis and scavenging activity in epithelial cells. *Mol Biol Cell* **12**, 2061-73.

Fish, K. N., Schmid, S. L. and Damke, H. (2000). Evidence that dynamin-2 functions as a signal-transducing GTPase. *J Cell Biol* **150**, 145-54.

Gampel, A., Moss, L., Jones, M. C., Brunton, V., Norman, J. C. and Mellor, H. (2006). VEGF regulates the mobilization of VEGFR2/KDR from an intracellular endothelial storage compartment. *Blood* **108**, 2624-31.

Garrett, W. S., Chen, L. M., Kroschewski, R., Ebersold, M., Turley, S., Trombetta, S., Galan, J. E. and Mellman, I. (2000). Developmental control of endocytosis in dendritic cells by Cdc42. *Cell* **102**, 325-34.

Gourlaouen, M., Welti, J. C., Vasudev, N. S. and Reynolds, A. R. (2013). Essential role for endocytosis in the growth factor-stimulated activation of ERK1/2 in endothelial cells. *J Biol Chem* **288**, 7467-80.

Herbert, S. P. and Stainier, D. Y. (2011). Molecular control of endothelial cell behaviour during blood vessel morphogenesis. *Nat Rev Mol Cell Biol* **12**, 551-64.

Holmes, D. I. and Zachary, I. C. (2008). Vascular endothelial growth factor regulates stanniocalcin-1 expression via neuropilin-1-dependent regulation of KDR and synergism with fibroblast growth factor-2. *Cell Signal* **20**, 569-79.

Ishii, N., Kuwano, R. and Watanabe, Y. G. (2003). [Possible involvement of Ankhzn, a novel protein possessing FYVE domain, in cellular endocytosis and autophagocytosis in vitro]. *Kaibogaku Zasshi* **78**, 53-8.

Karali, E., Bellou, S., Stellas, D., Klinakis, A., Murphy, C. and Fotsis, T. (2014). VEGF Signals through ATF6 and PERK to promote endothelial cell survival and angiogenesis in the absence of ER stress. *Mol Cell* **54**, 559-72.

Kerr, M. C. and Teasdale, R. D. (2009). Defining macropinocytosis. *Traffic* **10**, 364-71.

Koch, S., van Meeteren, L. A., Morin, E., Testini, C., Westrom, S., Bjorkelund, H., Le Jan, S., Adler, J., Berger, P. and Claesson-Welsh, L. (2014). NRP1 presented in trans to the endothelium arrests VEGFR2 endocytosis, preventing angiogenic signaling and tumor initiation. *Dev Cell* **28**, 633-46.

Koivusalo, M., Welch, C., Hayashi, H., Scott, C. C., Kim, M., Alexander, T., Touret, N., Hahn, K. M. and Grinstein, S. (2010). Amiloride inhibits macropinocytosis by lowering submembranous pH and preventing Rac1 and Cdc42 signaling. *J Cell Biol* **188**, 547-63.

Korff, T. and Augustin, H. G. (1999). Tensional forces in fibrillar extracellular matrices control directional capillary sprouting. *J Cell Sci* **112 (Pt 19)**, 3249-58.

Kuhling, L. and Schelhaas, M. (2014). Systematic analysis of endocytosis by cellular perturbations. *Methods Mol Biol* **1174**, 19-46.

Lajoie, P. and Nabi, I. R. (2010). Lipid rafts, caveolae, and their endocytosis. *Int Rev Cell Mol Biol* **282**, 135-63.

Lampugnani, M. G., Orsenigo, F., Gagliani, M. C., Tacchetti, C. and Dejana, E. (2006). Vascular endothelial cadherin controls VEGFR-2 internalization and signaling from intracellular compartments. *J Cell Biol* **174**, 593-604.

Lanahan, A., Zhang, X., Fantin, A., Zhuang, Z., Rivera-Molina, F., Speichinger, K., Prahst, C., Zhang, J., Wang, Y., Davis, G. et al. (2013). The neuropilin 1 cytoplasmic domain is required for VEGF-A-dependent arteriogenesis. *Dev Cell* **25**, 156-68.

Lanahan, A. A., Hermans, K., Claes, F., Kerley-Hamilton, J. S., Zhuang, Z. W., Giordano, F. J., Carmeliet, P. and Simons, M. (2010). VEGF Receptor 2 Endocytic Trafficking Regulates Arterial Morphogenesis. *Dev Cell*.

Lee, M. Y., Skoura, A., Park, E. J., Landskroner-Eiger, S., Jozsef, L., Luciano, A. K., Murata, T., Pasula, S., Dong, Y., Bouaouina, M. et al. (2014). Dynamin 2 regulation of integrin endocytosis, but not VEGF signaling, is crucial for developmental angiogenesis. *Development* **141**, 1465-72.

Macia, E., Ehrlich, M., Massol, R., Boucrot, E., Brunner, C. and Kirchhausen, T. (2006). Dynasore, a cell-permeable inhibitor of dynamin. *Dev Cell* **10**, 839-50.

Manickam, V., Tiwari, A., Jung, J. J., Bhattacharya, R., Goel, A., Mukhopadhyay, D. and Choudhury, A. (2011). Regulation of vascular endothelial growth factor receptor 2 trafficking and angiogenesis by Golgi localized t-SNARE syntaxin 6. *Blood* **117**, 1425-35.

Mayor, S. and Pagano, R. E. (2007). Pathways of clathrin-independent endocytosis. *Nat Rev Mol Cell Biol* **8**, 603-12.

McKay, M. M. and Morrison, D. K. (2007). Integrating signals from RTKs to ERK/MAPK. *Oncogene* **26**, 3113-21.

McMahon, H. T. and Boucrot, E. (2011). Molecular mechanism and physiological functions of clathrin-mediated endocytosis. *Nat Rev Mol Cell Biol* **12**, 517-33.

Mercer, J. and Helenius, A. (2009). Virus entry by macropinocytosis. *Nat Cell Biol* **11**, 510-20.

Miaczynska, M., Pelkmans, L. and Zerial, M. (2004). Not just a sink: endosomes in control of signal transduction. *Curr Opin Cell Biol* **16**, 400-6.

Monti, M., Donnini, S., Morbidelli, L., Giachetti, A., Mochly-Rosen, D., Mignatti, P. and Ziche, M. (2013). PKCepsilon activation promotes FGF-2 exocytosis and induces endothelial cell proliferation and sprouting. *J Mol Cell Cardiol* **63**, 107-17.

Mu, F. T., Callaghan, J. M., Steele-Mortimer, O., Stenmark, H., Parton, R. G., Campbell, P. L., McCluskey, J., Yeo, J. P., Tock, E. P. and Toh, B. H. (1995). EEA1, an early endosome-associated protein. EEA1 is a conserved alpha-helical peripheral membrane protein flanked by cysteine "fingers" and contains a calmodulin-binding IQ motif. *J Biol Chem* **270**, 13503-11.

Nakayama, M., Nakayama, A., van Lessen, M., Yamamoto, H., Hoffmann, S., Drexler, H. C., Itoh, N., Hirose, T., Breier, G., Vestweber, D. et al. (2013). Spatial regulation of VEGF receptor endocytosis in angiogenesis. *Nat Cell Biol* **15**, 249-60.

Olsson, A. K., Dimberg, A., Kreuger, J. and Claesson-Welsh, L. (2006). VEGF receptor signalling - in control of vascular function. *Nat Rev Mol Cell Biol* **7**, 359-71.

Papanikolaou, A., Papafotika, A. and Christoforidis, S. (2011). CD39 reveals novel insights into the role of transmembrane domains in protein processing, apical targeting and activity. *Traffic* **12**, 1148-65.

Parton, R. G. and del Pozo, M. A. (2013). Caveolae as plasma membrane sensors, protectors and organizers. *Nat Rev Mol Cell Biol* **14**, 98-112.

Pasula, S., Cai, X., Dong, Y., Messa, M., McManus, J., Chang, B., Liu, X., Zhu, H., Mansat, R. S., Yoon, S. J. et al. (2012). Endothelial epsin deficiency decreases tumor growth by enhancing VEGF signaling. *J Clin Invest* **122**, 4424-38.

Pelkmans, L., Bürli, T., Zerial, M. and Helenius, A. (2004). Caveolin-stabilized membrane domains as multifunctional transport and sorting devices in endocytic membrane traffic. *Cell* **118**, 767-80.

Platta, H. W. and Stenmark, H. (2011). Endocytosis and signaling. *Curr Opin Cell Biol* **23**, 393-403.

Salikhova, A., Wang, L., Lanahan, A. A., Liu, M., Simons, M., Leenders, W. P., Mukhopadhyay, D. and Horowitz, A. (2008). Vascular endothelial growth factor and semaphorin induce neuropilin-1 endocytosis via separate pathways. *Circ Res* **103**, e71-9.

Sawamiphak, S., Seidel, S., Essmann, C. L., Wilkinson, G. A., Pitulescu, M. E., Acker, T. and Acker-Palmer, A. (2010). Ephrin-B2 regulates VEGFR2 function in developmental and tumour angiogenesis. *Nature* **465**, 487-91.

Schenck, A., Goto-Silva, L., Collinet, C., Rhinn, M., Giner, A., Habermann, B., Brand, M. and Zerial, M. (2008). The endosomal protein Appl1 mediates Akt substrate specificity and cell survival in vertebrate development. *Cell* **133**, 486-97.

Schmees, C., Villasenor, R., Zheng, W., Ma, H., Zerial, M., Heldin, C. H. and Hellberg, C. (2012). Macropinocytosis of the PDGF beta-receptor promotes fibroblast transformation by H-RasG12V. *Mol Biol Cell* **23**, 2571-82.

Schmidt, F. I., Bleck, C. K., Helenius, A. and Mercer, J. (2011). Vaccinia extracellular virions enter cells by macropinocytosis and acid-activated membrane rupture. *EMBO J* **30**, 3647-61.

Schnatwinkel, C., Christoforidis, S., Lindsay, M. R., Uttenweiler-Joseph, S., Wilm, M., Parton, R. G. and Zerial, M. (2004). The Rab5 effector Rabankyrin-5 regulates and coordinates different endocytic mechanisms. *PLoS Biol* **2**, E261.

Sever, S., Damke, H. and Schmid, S. L. (2000). Garrotes, springs, ratchets, and whips: putting dynamin models to the test. *Traffic* **1**, 385-92.

Shvets, E., Ludwig, A. and Nichols, B. J. (2014). News from the caves: update on the structure and function of caveolae. *Curr Opin Cell Biol* **29**, 99-106.

Smith, D. D., Cohick, C. B. and Lindsley, H. B. (1997). Optimization of cellular ELISA for assay of surface antigens on human synoviocytes. *Biotechniques* **22**, 952-7.

Sorkin, A. and von Zastrow, M. (2009). Endocytosis and signalling: intertwining molecular networks. *Nat Rev Mol Cell Biol* **10**, 609-22.

Teis, D., Wunderlich, W. and Huber, L. A. (2002). Localization of the MP1-MAPK scaffold complex to endosomes is mediated by p14 and required for signal transduction. *Dev Cell* **3**, 803-14.

Tessneer, K. L., Pasula, S., Cai, X., Dong, Y., McManus, J., Liu, X., Yu, L., Hahn, S., Chang, B., Chen, Y. et al. (2014). Genetic reduction of vascular endothelial growth factor receptor 2 rescues aberrant angiogenesis caused by epsin deficiency. *Arterioscler Thromb Vasc Biol* **34**, 331-7.

Tiscornia, G., Singer, O. and Verma, I. M. (2006). Production and purification of lentiviral vectors. *Nat Protoc* **1**, 241-5.

Zhang, J., Reiling, C., Reinecke, J. B., Prislan, I., Marky, L. A., Sorgen, P. L., Naslavsky, N. and Caplan, S. (2012). Rabankyrin-5 interacts with EHD1 and Vps26 to regulate endocytic trafficking and retromer function. *Traffic* **13**, 745-57.

Zografou, S., Basagiannis, D., Papafotika, A., Shirakawa, R., Horiuchi, H., Auerbach, D., Fukuda, M. and Christoforidis, S. (2012). A complete Rab screening reveals novel insights in Weibel-Palade body exocytosis. *J Cell Sci* **125**, 4780-90.

Zouggari, Y., Ait-Oufella, H., Waeckel, L., Vilar, J., Loinard, C., Cochain, C., Récalde, A., Duriez, M., Levy, B. I., Lutgens, E. et al. (2009). Regulatory T cells modulate postischemic neovascularization. *Circulation* **120**, 1415-25.

FIGURE LEGENDS

Figure 1. VEGF introduces a clathrin- and dynamin-independent internalisation pathway for VEGFR2.

HUVECs treated with siRNAs against CHC were incubated with a mouse anti-VEGFR2 extracellular domain antibody at 4^0C, transferred to 37^0C and the receptor was allowed to internalise for 15 min, in the absence (**A**) or the presence (**B**) of VEGF and FITC-transferrin. Prior to fixation, membrane bound antibodies and transferrin were removed by acid wash and the internalised receptor was revealed by fluorescently labeled secondary antibodies, using confocal microscopy. Inhibition of transferrin uptake verified the effective inhibition of clathrin-mediated endocytosis. Quantification of VEGFR2 internalisation (relatively to initial VEGFR2

levels of non-stimulated cells) is shown on the right of immunofluorescence images (10 μm scale bars). The data shown are representative of 3 independent experiments (n=15 cells, mean ± S.D., ***P<0.001, t-test).

(**C**) CHC or caveolin-1 siRNAs treated HUVECs were incubated with VEGF for 15 min, transferred to 4^0C and surface proteins were labeled with cell impermeable biotin. Surface biotinylated proteins were pulled-down by streptavidin-beads and analysed by immunoblotting. Surface VEGFR2 was revealed using rabbit anti-VEGFR2 antibodies. Quantification of VEGFR2 is shown on the right of the immunoblots (n=3, mean ± S.D., one-way ANOVA, Dunnett).

(**D**) Quantitative ELISA-like assay of surface VEGFR2 in CHC or caveolin-1 knocked down cells upon induction with VEGF (30 min). Values represent the percentage (%) of the receptor that remains at the plasma membrane of stimulated cells, compared to the levels of quiescent cells. Data shown are representative of 3 independent experiments performed in quadruplicates (mean ± S.D., **P<0.01, one-way ANOVA, Dunnett).

Figure 2. VEGF induces the internalization of VEGFR2 in large endocytic vesicles.

(**A**) Live cell time-lapse video microscopy of HUVECs expressing GFP-actin and mCherry-VEGFR2. Magnified images show the VEGF-induced, progressive formation of an enlarged VEGFR2-positive vesicle (mCherry-VEGFR2), driven by extensive membrane ruffling (GFP-actin). Scale bar represents 3 μm. See also Movie S2.

(**B**) Analysis of the effect of VEGF on the number and fluorescence intensity of VEGFR2-positive vesicles. The number of VEGFR2-positive vesicles (lower graph) and the intensity of VEGFR2 fluorescence (upper graph) is presented (as fold of increase over constitutive internalisation) in relation to the size of the vesicles. The data shown are derived from 3 independent experiments (n=20 cells, mean ± S.D., ***P<0.001, **P<0.01 and *P<0.05, t-test).

(**C**) Electron microscopy analysis of VEGFR2-positive vesicles. Immunogold labeling of VEGFR2 (5 nm gold, arrowheads) on ultrathin cryosection of HUVECs stimulated with VEGF for 10 (*left*) or 20 min (*right*). Scale bars represent 500 nm. The graph on the right shows quantification of the number of gold particles (n=250) in vesicles below or above 0.2 μm, after 10 or 20 min of treatment with VEGF. The white bars show the number of gold particles in vesicles that have size <0.2 μm, while the black bars show the gold particles in large vesicles >0.2 μm (n=3, mean ± S.D., *P<0.05, **P<0.01, t-test).

Figure 3. VEGF induces a preferential internalization of VEGFR2 via macropinocytosis.

(**A**) Immunofluorescence microscopy analysis of VEGFR2 colocalization with dextran and Rabankyrin-5. HUVECs were incubated with an anti-VEGFR2 antibody at 4^0C and were

transferred to 37^{0}C for 15 min, in the presence of 70 kDa dextran, without (*top*) or with VEGF (*bottom*). Cells were acid washed, fixed and stained for endogenous Rabankyrin-5. The fold of induction of internalisation of VEGFR2, upon treatment with VEGF, is indicated in the inset text in the bottom left image (10 µm scale bars).

(**B**) Immunofluorescence microscopy analysis of VEGFR2 internalisation upon inhibition of macropinocytosis. Plasma membrane anti-VEGFR2 antibody labeled HUVECs were treated with vehicle (*top*) or EIPA (*middle*) or EIPA+dynasore (*bottom*) and stimulated with VEGF (15 min), in the presence of 70 kDa dextran. Cells were acid-washed, fixed and stained for endogenous Rabankyrin-5. Scale bars represent 10 µm. Quantification of the number and size of VEGFR2-positive vesicles is shown on the right of immunofluorescence images. The data shown are representative of 3 independent experiments (n=15 cells, mean ± S.D.)

(**C**) Quantitative ELISA-like assay of surface VEGFR2. Effect of inhibition of dynamin (by dynasore) or of macropinocytosis (by EIPA) or of dynamin and macropinocytosis (by EIPA+dynasore) on the internalisation of VEGFR2. HUVECs were treated for 30 min with vehicle or inhibitors, stimulated with VEGF (30 min) and assayed using surface ELISA. Data shown are representative of 3 independent experiments performed in quadruplicates (mean ± S.D., ***P<0.001, **P<0.01, one-way ANOVA, Dunnett).

Figure 4. Macropinocytosis of VEGFR2 is mediated by CDC42.

(**A**) HUVECs were treated with siRNAs against CDC42, incubated with a mouse anti-VEGFR2 extracellular domain antibody at 4^{0}C and transferred to 37^{0}C, where the receptor was allowed to internalise for 15 min, in the absence (left) or the presence (right) of VEGF and 70kDa dextran. Prior to fixation, membrane bound antibodies and dextran were removed by acid wash and the internalised receptor was revealed by incubation with fluorescently labeled secondary antibodies, using confocal microscopy. Quantification of VEGFR2 internalisation, from three independent experiments, is shown on the right of the immunofluorescence images (10 µm scale bars) (n=30 cells, mean ± S.D., ***P<0.001, t-test).

(**B**) HUVECs were treated with siRNAs against CDC42, incubated with VEGF for 15 min, transferred to 4^{0}C and surface proteins were labeled with cell-impermeable biotin. Surface biotinylated proteins were pulled-down by streptavidin-beads and analysed by immunoblotting. Surface VEGFR2 was revealed using rabbit anti-VEGFR2 antibodies. Quantification of VEGFR2 internalisation is shown on the right of the immunoblots (n=3, mean ± S.D., ***P<0.001, t-test).

(**C**) HUVECs were treated with siRNAs against CDC42, serum-starved for 2h, incubated with 100 µm cycloheximide for 30 min and stimulated with VEGF for the indicated time intervals.

Quantification of VEGFR2 levels is shown on the right of the immunoblots (n=4, mean ± S.D., ***P<0.001, two-way ANOVA, Bonferroni).

Figure 5. Clathrin-mediated endocytosis is not essential for VEGF signalling.
HUVECs transfected with siRNAs against clathrin heavy chain, or caveolin-1 (**A**), or dynamin 2 (**B**), were stimulated with VEGF and subjected to immunoblotting analysis using antibodies against ERK1/2 and Akt (phosphorylated or total). The efficiency of dynamin 2 knockdown was determined by semi-quantitative RT-PCR, 60h post-transfection of the cells. Levels were normalised to GAPDH. Bar graphs on the right show quantification of the immunoblots (n=3, mean ± S.D., two-way ANOVA, Bonferroni).

Figure 6. Macropinocytosis is critical for VEGF signalling and *in vitro* angiogenic responses.
(**A**) Treatment with EIPA or knockdown of CDC42 inhibits VEGF-induced activation of ERK1/2 and Akt. HUVECs treated with vehicle or EIPA (*upper panels*) or HUVECs treated with siRNAs against CDC42 (*bottom panels*) were stimulated with VEGF and subjected to immunoblotting analysis using antibodies against ERK1/2 and Akt (phosphorylated or total). Bar graphs on the right show quantification of the immunoblots (n=3, mean ± S.D., *P<0.05, ***P<0.001, two-way ANOVA, Bonferroni).
(**B**) VEGF-induced endothelial cell sprouting is inhibited by EIPA or knockdown of CDC42. (*left*) HUVEC spheroids were embedded in 3D collagen gels and were treated with vehicle or EIPA in the presence of VEGF for 16h (*upper panel*). Similarly, HUVEC spheroids derived from cells treated with siRNAs against CDC42, CHC, or dynamin 2 were treated with VEGF as above (*lower panel*). Images are representative of 3 independent experiments. Quantification of the mean sprout length of 8 randomly selected spheres for each experimental setting is shown on the right of the images (mean ± S.D., **P<0.01, ***P<0.001, t-test).
(**C**) Knockdown of CDC42 or treatment with EIPA abolishes VEGF-induced migration of endothelial cells. Confluent HUVEC cultures of cells treated with siRNAs against CDC42, CHC, or dynamin 2, or, EIPA-treated cells (30 min), were scratched linearly with a pipette tip and stimulated with VEGF for 14h. VEGF untreated cells were analysed in parallel. The bar graph depicts the average migration of the cells towards the centre of the wound (distance in μm) (n=12 injury areas from 3 independent experiments, mean ± S.D., ***P<0.001, t-test).
(**D**) VEGF-induced survival of endothelial cells is CDC42-dependent. The cell viability of HUVECs treated with siRNAs against CDC42, CHC, or dynamin 2, was assessed by the MTT assay. Bar graph depicts % fold of VEGF-induced survival of HUVECs relatively to

VEGF-untreated cells. Values are representative of three independent experiments carried out in triplicates (mean± S.D., *P<0.05, ***P<0.001, t-test).

Figure 7. Schematic representation (model) of constitutive and stimulated internalisation routes of VEGFR2 and their role in VEGFR2 function. (*left*) At steady state, quiescent VEGFR2 is internalised via the clathrin-dependent internalisation route (CME). (*right)* In the presence of VEGF, VEGFR2 is endocytosed via both CME and macropinocytosis, the later being the preferred route. Macropinocytosis of VEGFR2 is mediated by CDC42 and is critical for VEGF-induced signalling.
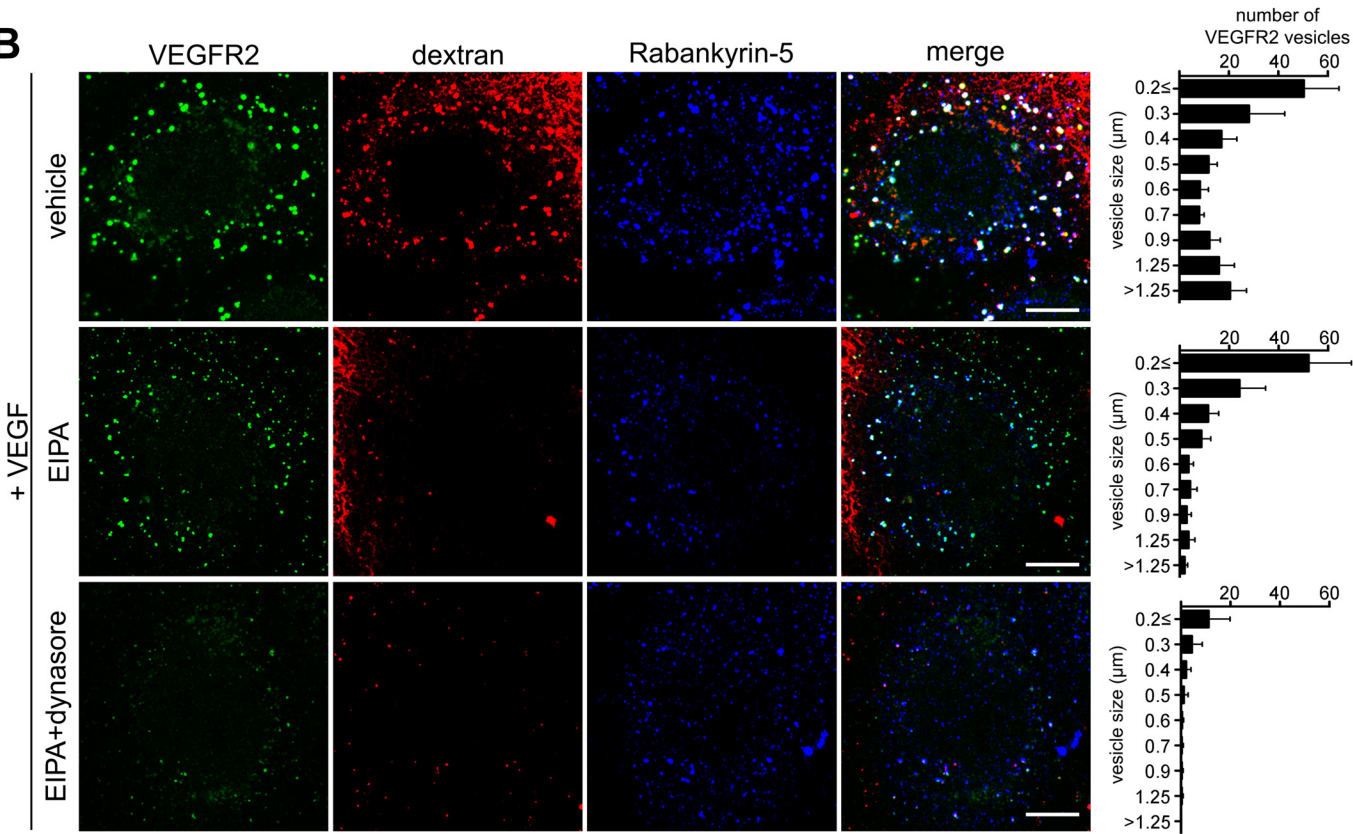
Figure 1

Figure 2

A

VEGFR2-mCherry-actin-GFP

live-cell time lapse video microscopy

B

C

Figure 3

A

	VEGFR2	dextran	Rabankyrin-5	merge
constitutive uptake	internalization=1x			
+VEGF	internalization=2.5x (±0.25)			

B

+ VEGF: vehicle, EIPA, EIPA+dynasore

number of VEGFR2 vesicles

vesicle size (µm): 0.2≤, 0.3, 0.4, 0.5, 0.6, 0.7, 0.9, 1.25, >1.25

C

ELISA-like assay of surface VEGFR2

% surface VEGFR2

initial levels (-VEGF), vehicle, dynasore, EIPA, EIPA+dynasore

+ VEGF

** *** ***

Figure 4

A

	VEGFR2	dextran	merge
scrambled			
CDC42 knock down			

B

pull down of surface biotinylated proteins

C

Figure 5

A

scrambled   CHC k.d.   cav1 k.d.

p-ERK1/2
p-Akt
ERK1/2
Akt
CHC
cav-1
EEA1

0 10 20 30   0 10 20 30   0 10 20 30

time of treatment with VEGF (min)

B

scrambled   dyn2 k.d.

p-ERK1/2
p-Akt
ERK1/2
Akt

0 10 20 30   0 10 20 30

time of treatment with VEGF (min)

scrambled   dyn2 k.d.

dyn2
GAPDH

Figure 6

Figure 7